

NJC

New Journal of Chemistry

Accepted Manuscript

A journal for new directions in chemistry

This article can be cited before page numbers have been issued, to do this please use: N. K. Oklu and B. C.E. Makhubela, *New J. Chem.*, 2020, DOI: 10.1039/D0NJ01811B.



This is an Accepted Manuscript, which has been through the Royal Society of Chemistry peer review process and has been accepted for publication.

Accepted Manuscripts are published online shortly after acceptance, before technical editing, formatting and proof reading. Using this free service, authors can make their results available to the community, in citable form, before we publish the edited article. We will replace this Accepted Manuscript with the edited and formatted Advance Article as soon as it is available.

You can find more information about Accepted Manuscripts in the [Information for Authors](#).

Please note that technical editing may introduce minor changes to the text and/or graphics, which may alter content. The journal's standard [Terms & Conditions](#) and the [Ethical guidelines](#) still apply. In no event shall the Royal Society of Chemistry be held responsible for any errors or omissions in this Accepted Manuscript or any consequences arising from the use of any information it contains.

Chemoselective and efficient catalytic hydrogenation of furfural by iridium and ruthenium half-sandwich complexes

Novisi K. Oklu^a and Banothile C. E. Makhubela^{a*}

^a *University of Johannesburg, Research Centre for Synthesis and Catalysis, Department of Chemical Sciences, Auckland Park 2006, Johannesburg, South Africa.*

*E-mail: bmakhubela@uj.ac.za

ABSTRACT

The efficient hydrogenation reaction of furfural (FFR) to furfuryl alcohol (FFA) was achieved with new pyridyl-imine iridium(III) and ruthenium(II) complexes as catalyst precursors. The hydrogenation of furfural yielded furfuryl alcohol selectively with a turnover number (TON) of 2961 and turnover frequency (TOF) of 1481 h⁻¹. The reactions were performed with formic acid as the source of hydrogen using a catalyst loading as low as 0.025 mol% and Et₃N as base. The catalyst remained active for up to seven consecutive catalyst reuse cycles. Iridium outperformed the ruthenium analogues in terms of selectivity. Iridium hydride species were detected, during *in situ* ¹H NMR spectroscopy studies, and are believed to be the active catalytic species. A mechanism of the hydrogenation reaction has hence been proposed.

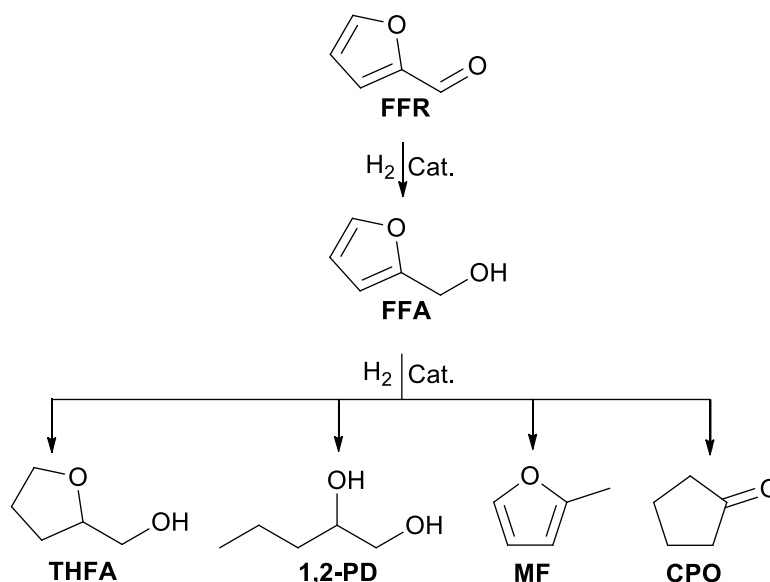
KEYWORDS

iridium(III), ruthenium(II), half-sandwich complexes, furfural, furfuryl alcohol, hydrogenation

1. INTRODUCTION

Depleting fossil resources and growing environmental concerns, has stoked the quest for renewable resources to synthesize chemicals and liquid fuels. Biomass is a promising alternative to the current fossil resources as it is readily available and renewable.¹⁻³ Valorisation of biomass is usually aimed at producing platform molecules, which can further be transformed into useful chemicals and fuels.⁴ The US Department of Energy (DOE) was

the first to come up with a list of platform molecules in 2004⁵. However Bozell and Peterson⁶ revisited this list the following year and updated the list to include sugars (glucose, xylose), furans (5-hydroxymethylfurfural, furfural), polyols (sorbitol, glycerol, xylitol) and organic acids (lactic, succinic, levulinic acids).⁴ One of the important platform molecules which features in this updated list, furfural (FFR), has an annual global demand of around 30 kton/year.⁷ It is produced from the hydrolysis of xylan, found in the hemicellulose part of lignocellulosic biomass.⁸ It serves as a raw material for the production of a variety of valuable chemicals including furfuryl alcohol (FFA), which in turn is used to produce fine chemicals and products such as tetrahydrofurfuryl alcohol (THFA), 1,2-pentanediol (1,2-PD), 2-methylfuran (MF), cyclopentanone (CPO) thermosetting resins, vitamin C, lysine and lubricants.⁹ FFA is synthesized by the hydrogenation of the aldehyde group in FFR as shown in **Scheme 1**.¹⁰



Scheme 1: Hydrogenation products of FFR⁹

Commercial production of FFA uses a copper chromite catalyst, high temperatures and high pressures of hydrogen gas. This method of production is unfavourable due to the toxicity of the chromite catalyst and the explosive nature of hydrogen gas at high temperature and pressure.¹¹ Due to this, focus has been shifted to catalyst systems that use alternative less toxic metal catalysts (based on Pd, Pt, Ru and Ir) while some reports use other safer sources of hydrogen like isopropanol and formic acid.^{12–17} The hydrogenation of aldehydes as well as ketones was first described in 1925 by Meerwein-Ponndorf-Verley *via* transfer hydrogenation and since then a considerable amount of progress has been made in the field of transfer

hydrogenation.^{18–20} Catalyst systems commonly used for transfer hydrogenation reactions are less efficient in reducing aldehydes and also have difficulties in controlling the chemoselectivity to the alcohol product.²¹

Many homogeneous catalytic systems such as Ru and Ir complexes^{22–25} which have been used in the hydrogenation of biomass derivatives have been reported. In our previous work, we successfully hydrogenated levulinic acid into gamma-valerolactone, another important platform chemical obtained from lignocellulose, using half-sandwich ruthenium complexes as catalyst precursors. Complete conversions and high selectivities to gamma-valerolactone was achieved in a solvent-free system with formic acid as the hydrogen source.^{26–28} There are few reports on the conversion of furfural to furfural alcohol with homogenous Ru and Ir complexes with relatively good yield (**Figure 1**). Amongst these, most use hydrogen gas, while some need the presence of other additives. In others, difficult-to-handle supporting ligands such as trialkyl phosphines are used to stabilize the catalyst precursors and there are no studies done on the recyclability of the catalysts.^{15,29–33} Still, the selectivity for FFA is low when using these catalytic systems.

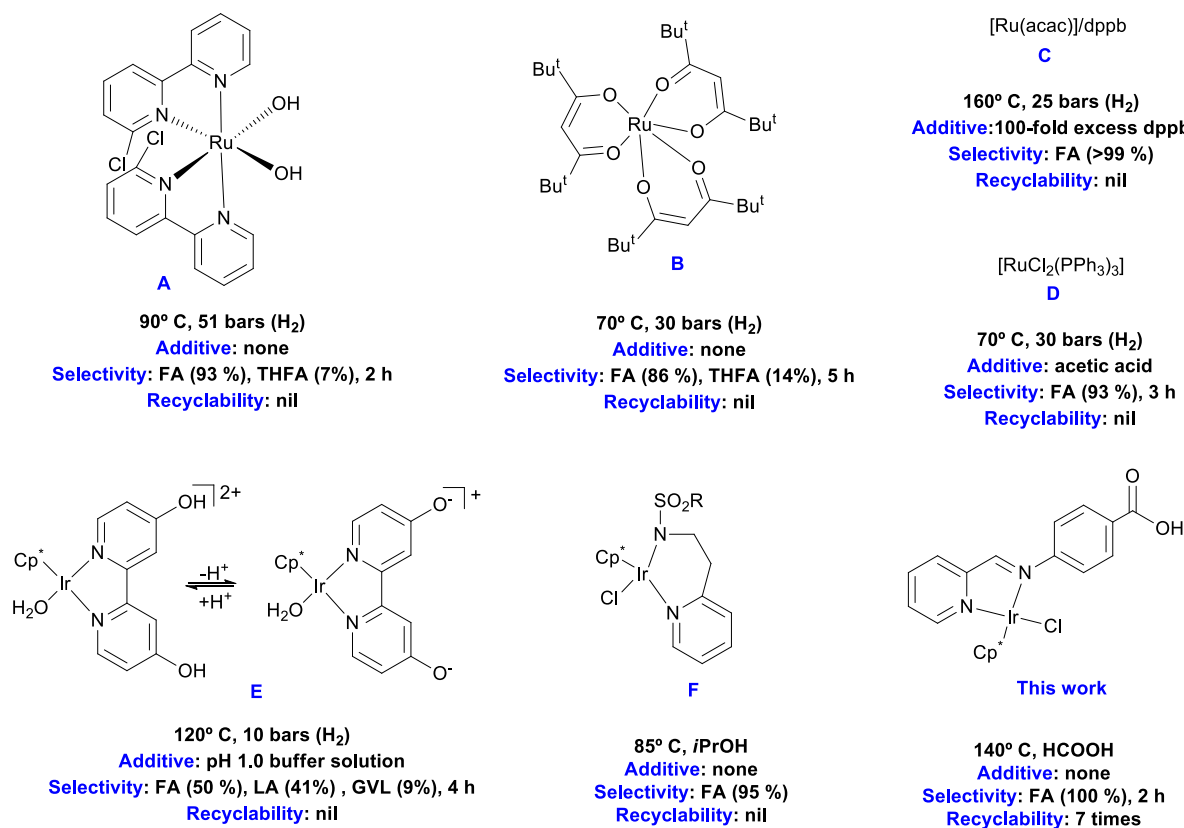


Figure 1: Homogeneous Ruthenium and Iridium catalysts used in the hydrogenation of furfural to furfuryl alcohol

1
2
3
4
5
6
7
8
9
10
11
12
13
14
15
16
17
18
19
20
21
22
23
24
25
26
27
28
29
30
31
32
33
34
35
36
37
38
39
40
41
42
43
44
45
46
47
48
49
50
51
52
53
54
55
56
57
58
59
60

Wu *et al.*, for instance reported very high turnover numbers ($13\ 877\ \text{h}^{-1}$) in conversion of FFR to FFA using an iridium half-sandwich catalyst (**Figure 1E**). However, to achieve these results, they needed a phosphate buffer solution as an additive in addition to 10 bars of hydrogen gas. There was also no further study done to show the recyclability of their catalysts.¹⁵ O'Connor and co-workers also, reported the conversion of FFR to FFA in 95 % yield within a short reaction time, using an iridium half-sandwich complex as the catalyst (**Figure 1F**) and 2-propanol as both solvent and hydrogen source. They used a high catalyst loading of 1 mol% and also didn't report on the recyclability of their catalyst.³⁰ It is important to develop recyclable homogeneous catalysts, from ligands that are easy to handle and synthesize (preferably one step) which require no further additives and solvents to synthesize FFA selectively from FFR.

Herein, we report the synthesis of half-sandwich iridium(III) and ruthenium(II) complexes and their utilization as catalyst precursors in the chemoselective hydrogenation of FFR into FFA. These complexes do not require hydrogen gas and do not need further additive to achieve efficient hydrogenation.

2. EXPERIMENTAL

2.1 General Information

4-aminobenzoic acid (99%), 2-pyridinecarboxylic acid (99%), 2-quinolinecarboxaldehyde (97%), dichloro(p-cymene)ruthenium(II)dimer, iridium cyclopentadiene dimer, Furfural (97%), Triethylamine, Sodium hexafluorophosphate (98%) and formic acid (95%) were all purchased from Sigma-Aldrich and were used as supplied. All solvents used were of analytical grade and were dried using MBRAUN SPS-800 solvent drying system. ¹H NMR (400 MHz) and ¹³C{¹H} NMR (100 MHz) spectra were recorded on a Bruker-400 MHz spectrometer and values were reported relative to tetramethylsilane ($\delta\ 0.0$) as internal standard. FT-IR spectra were recorded using a Perkin Elmer FT-IR Spectrum BX-ATR. Elemental analyses were performed on a Thermo Scientific FLASH 2000 CHNS-O analyzer. HR-MS (ESI) spectra were recorded on a Waters Synapt G2 spectrometer. Ligands **L1**, **L2** and complexes **1** and **2** were synthesized following reported literature methods.²⁶

2.2 General Procedure for the synthesis of complexes 1 to 4

View Article Online
DOI: 10.1039/D0NJ01811B

2.2.1 [Ru(*p*-cymene)Cl(L1)]Cl (1)

Complex **1** was synthesized according to reported literature methods.²⁶ Yield: (270 mg, 93.9 %); M.p: decomposes without melting (onset at 180 °C); FT-IR ($\nu_{\max}/\text{cm}^{-1}$): 3380 b (OH), 1702 s (C=O), 1600 s (HC=N); ¹H NMR (400 MHz, MeOD-d₄, 25 °C, δ , ppm): 9.53 (d, ³J_{HH} = 5.60 Hz, 1H, pyr-CH), 8.84 (s, 1H, imine-CH), 8.31 – 8.25 (m, 4H, pyr-CH, pyr-CH, aromatic-CH), 7.89 (d, ³J_{HH} = 8.40 Hz, 2H, aromatic-CH), 7.86 (t, ³J_{HH} = 5.60 Hz, 1H, pyr-CH), 6.00 (d, ³J_{HH} = 6.00 Hz, 1H, *p*-cym-CH), 5.69 (d, ³J_{HH} = 6.00 Hz, 1H, *p*-cym-CH), 5.64 (d, ³J_{HH} = 6.00 Hz, 1H, *p*-cym-CH), 5.50 (d, ³J_{HH} = 6.40 Hz, 1H, *p*-cym-CH), 2.60 (m, ³J_{HH} = 7.20 Hz, 1H, *p*-cym-CH(CH₃)₂), 2.25 (s, 3H, *p*-cym-CH₃), 1.09 (d, ³J_{HH} = 6.80 Hz, 6H, *p*-cym-CH₃); ¹³C{¹H} NMR (100 MHz, DMSO-d₆, 25 °C, δ , ppm): 206.41 (-COOH), 168.94 (imine-C=N), 166.48 (pyridyl-C=N), 156.15 (pyr-CH), 154.72, 154.38 (aromatic-C(COOH)), 139.94 (pyr-CH), 130.64 (aromatic-CH), 130.50 (pyr-CH), 129.11 (pyr-CH), 122.76 (aromatic-CH), 105.24 (*p*-cym-C(CH₃)), 103.71, 86.67 (*p*-cym-CH), 86.00 (*p*-cym-CH), 84.87 (*p*-cym-CH, *p*-cym-CH), 30.45 (*p*-cym-C(CH₃)₂), 21.67 (*p*-cym-CH₃, *p*-cym-CH₃), 18.26 (*p*-cym-CH₃); CHN-calculated: (51.88 % C, 4.56 % H, 5.26 % N), CHN-obtained: (52.26 % C, 4.53 % H, 4.96 % N); HR-MS (ESI⁺) [C₂₃H₂₄ClN₂O₂Ru]⁺ calculated, *m/z* = 497.0570 [M]⁺, found, *m/z* = 497.0570 [M]⁺; Solubility: water, methanol, ethanol.

2.2.2 Synthesis of [Ru(*p*-cymene)Cl(L2)]Cl (2)

Complex **2** was synthesized according to reported literature methods.²⁶ Yield: (193 mg, 91.90 %); M.p: decomposes without melting (onset at 187 °C); FT-IR ($\nu_{\max}/\text{cm}^{-1}$): 3387 b (OH), 1706 s (C=O), 1593 s (HC=N), 1513 w (C=N); ¹H NMR (400 MHz, MeOD-d₄, 25 °C, δ , ppm): 9.09 (s, 1H, imine-CH), 8.85 (d, ³J_{HH} = 8.40 Hz, 1H, quin-CH), 8.82 (d, ³J_{HH} = 8.80 Hz, 1H, quin-CH), 8.33 (d, ³J_{HH} = 8.40 Hz, 1H, quin-CH), 8.32 (d, ³J_{HH} = 8.40 Hz, 2H, aromatic-CH), 8.28 (d, ³J_{HH} = 8.40 Hz, 1H, quin-CH), 8.20 (t, ³J_{HH} = 7.60 Hz, 1H, quin-CH), 8.06 (d, ³J_{HH} = 8.80 Hz, 2H, aromatic-CH), 8.01 (t, ³J_{HH} = 7.20 Hz, 1H, quin-CH), 6.03 (d, ³J_{HH} = 6.40 Hz, 1H, *p*-cym-CH), 5.89 (d, ³J_{HH} = 6.00 Hz, 1H, *p*-cym-CH), 5.77 (d, ³J_{HH} = 6.40 Hz, 1H, *p*-cym-CH), 5.32 (d, ³J_{HH} = 6.00 Hz, 1H, *p*-cym-CH), 2.38 (m, ³J_{HH} = 7.20 Hz, 1H, *p*-cym-CH(CH₃)₂), 2.29 (s, 3H, *p*-cym-CH₃), 0.99 (d, ³J_{HH} = 6.80 Hz, 3H, *p*-cym-CH₃), 0.84 (d, ³J_{HH} = 6.80 Hz, 3H, *p*-cym-CH₃); ¹³C{¹H} NMR (100 MHz, DMSO-d₆, 25 °C, δ , ppm): 206.92 (-COOH), 170.34 (imine-C=N), 166.98 (pyridyl-C=N), 156.09, 155.55 (aromatic-C(COOH)), 148.92, 141.37 (quin-CH), 133.93 (quin-CH), 132.51, 131.27

(aromatic-CH), 130.99 (quin-CH), 129.80 (quin-CH, quin-CH), 125.39 (quin-CH), 123.23 (aromatic-CH), 106.01 (*p*-cym-C(CH₃)), 105.54, 87.01 (*p*-cym-CH), 86.82 *p*-cym-CH), 85.98 (*p*-cym-CH), 85.09 (*p*-cym-CH), 30.95 (*p*-cym-C(CH₃)₂), 22.51 (*p*-cym-CH₃), 21.43 (*p*-cym-CH₃), 18.78 (*p*-cym-CH₃); CHN-calculated: (55.67 % C, 4.50 % H, 4.81 % N), CHN-obtained: (56.00 % C, 4.56 % H, 4.75 % N); HR-MS (ESI⁺) [C₂₇H₂₆ClN₂O₂Ru]⁺ calculated, *m/z* = 547.0726 [M]⁺, found, *m/z* = 547.0725 [M]⁺; Solubility: water, methanol, ethanol.

2.2.3 [Ir(Cp*)Cl(L1)][PF₆] (3)

Ligand **L1** (40.72 mg, 0.18 mmol) and [IrCl₂Cp*]₂ (71.70 mg, 0.09 mmol) was stirred in dry methanol (20 ml) for 30 mins, followed by the addition of NaPF₆ (33.13 mg, 0.18 mmol). The solution was left to stir at 25 °C for 24 h. The solvent was removed via vacuum after which the orange solid formed was further dissolved in acetone. The resulting solution was filtered with a microfilter and the acetone removed under vacuum. After vacuum drying the solid overnight, a bright orange solid was obtained. Yield: 88 mg (66.60 %); FT-IR (ν_{max}/cm⁻¹): 1681 s (C=O), 1603 w (HC=N), 1561 w (C=N); ¹H NMR (400 MHz, DMSO-d₆, 25°C, ppm): δ 9.44 (s, 1H, imine-CH), δ 9.07 (d, ³J_{HH} = 5.20 Hz, 1H, pyr-CH), δ 8.45 (d, ³J_{HH} = 7.20 Hz, 1H, pyr-CH), δ 8.36 (t, ³J_{HH} = 7.60 Hz, 1H, pyr-CH), δ 8.19 (d, ³J_{HH} = 8.40 Hz, 2H, aromatic-CH), δ 7.96 (t, ³J_{HH} = 6.40 Hz, 1H, pyr-CH), δ 7.77 (d, ³J_{HH} = 8.40 Hz, 2H, aromatic-CH), δ 1.42 (s, 15H, Cp*-CH); ³¹P{¹H} NMR (161 MHz, DMSO-d₆, 25°C, ppm): δ -131.02 to -152.98 (m, 1P), ¹⁹F{¹H} NMR (376 MHz, DMSO-d₆, 25°C, ppm): δ -69.20 (s, 3F), δ -71.09 (s, 3F); CHN-calculated: (37.63% C, 3.43% H, 3.82% N), CHN-obtained: (38.01% C, 3.56% H, 3.76% N); HR-MS (ESI⁺) [C₂₃H₂₅ClN₂O₂Ir]⁺ calculated, *m/z* = 589.1234 [M]⁺, found, *m/z* = 589.1229 [M]⁺; Solubility: DMSO, acetone, methanol and ethanol.

2.2.4 [Ir(Cp*)Cl(L2)][PF₆] (4)

[IrCl₂Cp*]₂ (71.70 mg, 0.09 mmol) was stirred in dry methanol (20 ml) for about 10 mins followed by the addition of ligand **L2** (49.74 mg, 0.18 mmol). The mixture was allowed to stir for 30 mins before the addition of NaPF₆ (33.13 mg, 0.18 mmol). The solution was left to stir at 25 °C for 24 h. After 24 h, the resulting solution was filtered with a microfilter and the methanol removed via vacuum to afford a dark brown solid which was dried overnight under vacuum. Yield: 111 mg (78.64 %); FT-IR (ν_{max}/cm⁻¹): 1689 s (C=O), 1600 w (HC=N), 1516 w (C=N); ¹H NMR (400 MHz, DMSO-d₆, 25°C, ppm): δ 13.37 (s, 1H, COOH), δ 9.72 (s, 1H, imine-CH), δ 8.92 (d, ³J_{HH} = 8.40 Hz, 1H, quin-CH), δ 8.43 (d, ³J_{HH} = 8.00 Hz, 1H, quin-

CH), δ 8.36 (d, $^3J_{\text{HH}} = 8.80$ Hz, 1H, quin-CH), δ 8.30 (d, $^3J_{\text{HH}} = 8.40$ Hz, 1H, quin-CH), δ 8.18 (d, $^3J_{\text{HH}} = 8.40$ Hz, 2H, aromatic-CH), δ 8.15 (t, $^3J_{\text{HH}} = 8.80$ Hz, 1H, quin-CH), δ 8.01 (d, $^3J_{\text{HH}} = 8.40$ Hz, 2H, aromatic-CH), δ 7.97 (t, $^3J_{\text{HH}} = 7.60$ Hz, 1H, quin-CH), δ 1.30 (s, 15H, Cp*-CH); $^{31}\text{P}\{^1\text{H}\}$ NMR (161 MHz, DMSO- d_6 , 25°C, ppm): δ -135.41 to -157.36 (m, 1P), $^{19}\text{F}\{^1\text{H}\}$ NMR (376 MHz, DMSO- d_6 , 25°C, ppm): δ -69.20 (s, 3F), δ -71.09 (s, 3F); CHN-calculated: (41.36% C, 3.47% H, 3.57% N), CHN-obtained: (40.94% C, 3.61% H, 3.46% N); HR-MS (ESI $^+$) [$\text{C}_{27}\text{H}_{27}\text{ClN}_2\text{O}_2\text{Ir}$] $^+$ calculated, $m/z = 639.1390$ [M] $^+$, found, $m/z = 639.1395$ [M] $^+$; Solubility: DMSO, acetone, methanol and ethanol.

2.3 General procedure for hydrogenation reactions

Furfural (20 mmol), formic acid (20 mmol), catalyst (0.02 mmol / 0.1 mol %), and triethylamine (20 mmol) were added to an autoclave reactor. The mixture was heated to the desired temperature after purging four times with nitrogen gas. The mixture was then left to stir for the required length of time. At the end of the reaction, the reactor vessel was cooled and the gas generated released. A sample of the mixture was then analysed by ^1H NMR spectroscopy.

2.4 Crystal data collection, structure resolution and refinement

Single crystals suitable for X-ray diffraction analysis for complex **3** were grown and used to determine the structure for the complex. In a typical experiment, an orange crystal of **3** with approximate dimensions 0.70 x 0.27 x 0.20 mm 3 was selected under ambient conditions. The crystal was mounted in a stream of cold nitrogen at 100 K and centred in the X-ray beam using a video camera on the diffractometer. The crystal evaluation and data collection were performed using Quazar multi-layer optics monochromated Mo K α radiation ($\lambda = 0.71073$ Å) on a Bruker APEX-II CCD diffractometer and APEX III control software. All X-ray diffraction measurements were performed at 100 K and diffractometer to crystal distance of 4.00 cm. Data reduction was performed using SAINT+, and the intensities were corrected for absorption using SADABS.³⁴ Using the Olex2 software,³⁵ the structure was solved with the ShelXT³⁶ structure solution program using Intrinsic Phasing and refined with the ShelXL³⁷ refinement package using Least Squares minimisation. All non-hydrogen atoms were refined with anisotropic displacement coefficients. All hydrogen atoms were placed in geometrically

1
2
3 idealised positions and constrained to ride on their parent atoms. Crystallographic data has View Article Online
DOI: 10.1039/D0NJ01811B
4 been deposited with the Cambridge Crystallographic Data Centre with CCDC 1833342.

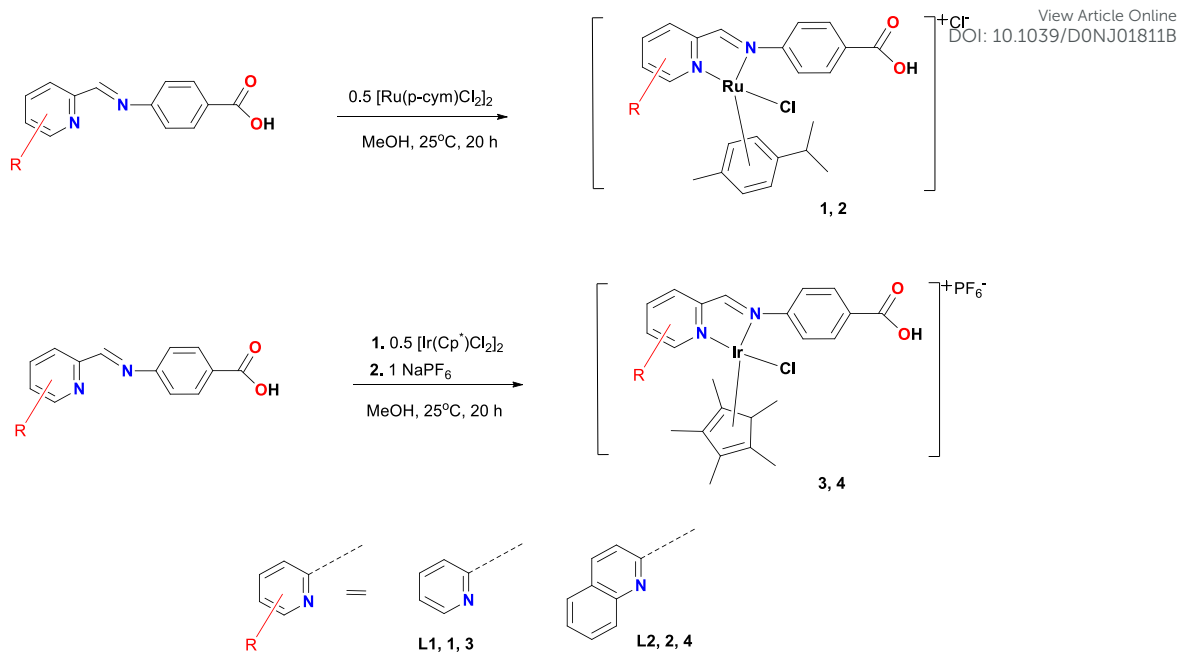
5
6 Copies of this information may be obtained free of charge from the Director, CCDC, 12
7 Union Road, Cambridge, CB2 1EZ, UK (fax: +44 1223 336063; deposit@ccdc.cam.ac.uk or
8 http://www.ccdc.cam.ac.uk).
9
10
11
12
13
14

15 3. RESULTS AND DISCUSSIONS

16 3.1 Synthesis of catalysts

17
18 The four complexes were characterised using ^1H and $^{13}\text{C}\{^1\text{H}\}$ NMR spectroscopy, elemental
19 analysis (CHN), infrared spectroscopy and mass spectrometry. The ^1H NMR spectra (**Figures**
20 **S1-S4**) of the complexes show significant shifts of the signal for the protons adjacent to the
21 pyridyl nitrogen as well as those of the imine protons. These shifts confirm the coordination
22 of both nitrogen atoms to the metal centres. For the ruthenium complexes **1** and **2**, a chloride
23 was displaced upon coordination and serves as the counter ion to stabilize the complex.
24 However, for the iridium analogues, complexes **3** and **4**, NaPF_6 was used to abstract a
25 chloride for successful bi-dentate coordination, where PF_6^- anion serves as the counter ion to
26 the complexes. The $[\text{M}]^+$ peaks, which correspond to the cationic part of the complexes, were
27 observed in the mass spectra (**Figures S5-S8**) of complexes **1** to **4**.
28
29
30
31
32
33
34
35
36
37
38
39
40
41
42
43
44
45
46
47
48
49
50
51
52
53
54
55
56
57
58
59
60

Single crystals suitable for XRD analysis were obtained for the iridium complex **3**.
Crystallization of **3** was performed by dissolving 5 mg of **3** in a vial containing about 1 ml
acetone. The vial was closed with a needle pierced lid and kept at room temperature to allow
slow evaporation. After a week, shiny orange prismatic crystals were obtained. The crystal
data and structure refinement parameters for **3** are presented in **Table 2**. The complex
crystallized in the $\text{P}2_1/\text{c}$ space group in a monoclinic crystal system. The crystal structure
obtained (**Figure 2**), confirmed the successful abstraction of one chloride from the iridium
metal centre to allow the successful coordination of a nitrogen atom to the iridium metal. The
structure also shows the cyclopentadiene η^5 -bonded to the iridium metal centre, causing the
complex to assume a piano-stool structure about the metal centre. Selected bond distances
and angles of **3** have been shown as captions under the molecular structure.



Scheme 2: Outline for the synthesis of complexes **1** to **4**.

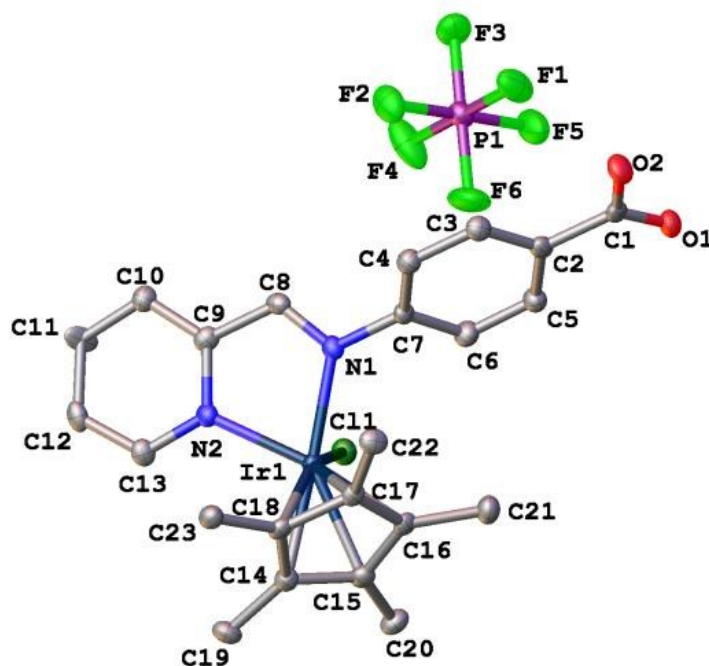


Figure 2: Molecular structure of **3** (hydrogen atoms removed for clarity). Selected bond lengths (Å) and bond angles (°): Ir(1)–Cl(1), 2.3843(11); Ir(1)–N(1), 2.084(4); Ir(1)–N(2), 2.115(4); N(1)–C(7), 1.431(6); N(1)–C(8), 1.284(7); N(1)–Ir(1)–Cl(1), 83.79(11); N(2)–Ir(1)–Cl(1), 85.74(12); N(1)–Ir(1)–N(2), 76.09(16)

The imine C=N bond remains intact as can be seen from the shorter bond length of the N(1)–C(8) bond (1.284(7) Å) as compared to that of the N(1)–C(7) bond (1.431(6) Å). The Ir–Cl bond length (2.3843(11) Å) and the two Ir–N bond lengths (2.115(4) and 2.084(4) Å) that were recorded for **3** are in accordance with those reported in literature.³⁸

3.2 Hydrogenation of FFR to FFA

In the preliminary hydrogenation studies, 20 mmol of FFR was reacted with 10 mmol of triethylamine base and 20 mmol formic acid at a 0.1 mol% catalyst loading for 10 h (**Table 1**). At these conditions, all catalysts gave 100% conversions of FFR. Catalysts **1**, **2** and **3** gave FFA selectivities of 89%, 83% and 99% respectively whereas **4** gave 100% selectivity (**Table 1**, entries 1-4). In an attempt to select the best performing catalyst, the reactions were repeated as before but for 6 h. Again, all catalysts gave 100% conversions with varied selectivities except for **4** which maintained 100% selectivity (**Table 1**, entries 5-8). The time was further reduced to 2 h and at this time, only **4** maintained 100% conversion and selectivity (**Table 1**, entries 9-12). From this preliminary study, it can be observed that iridium catalysts gave higher FFA selectivities than their ruthenium counterparts. The secondary product, mostly formed from the use of **1** and **2** was identified as difurfuryl ether (DFE), as was proven with ¹H NMR spectroscopy (**Figure S9**). The formation of DFE from FFA has been seen with heterogeneous catalysts in molecular hydrogen driven FFR hydrogenation reactions.¹² It was interesting to observe the formation of this product for the first time under transfer hydrogenation. We were able to optimize the reaction to achieve only up to <10% yield of DFE with the ruthenium complexes. Having established catalyst **4**'s better performance and selectivity in the series, this catalyst was used for further optimization of other parameters.

Table 1: Hydrogenation of FFR to FFA.View Article Online
DOI: 10.1039/D0NJ01811B

Entry	Catalyst	Time (h)	FFR Conversion (%) ^a	FFA Selectivity (%) ^a	DFE Selectivity (%) ^a	TON ^b	TOF (h ⁻¹) ^c
1	1	10	100	89	11	890	89
2	2	10	100	83	17	830	83
3	3	10	100	99	1	990	99
4	4	10	100	100	0	1000	100
5	1	6	100	92	8	920	142
6	2	6	100	86	14	860	127
7	3	6	100	99	1	990	158
8	4	6	100	100	0	1000	167
9	1	2	65	100	0	650	325
10	2	2	98	93	7	911	456
11	3	2	98	99	1	970	485
12	4	2	100	100	0	1000	500

Conditions: FFR (20 mmol), formic acid (20 mmol), catalyst (0.02 mmol), base (10 mmol), 140 °C.

[a] Conversion and Selectivity determined by NMR spectroscopy. [b] TON = moles of FFA / moles of catalyst. [c] TOF = TON / time.

3.2.1 Conversion as a function of amount of base

An interesting observation was made in our previous work in synthesizing gamma-valerolactone from bio-based levulinic acid,²⁶ where catalytic amounts of triethylamine base were enough to hydrogenate levulinic acid, using formic acid as the hydrogen source. This

 1
2
3
4
5
6
7
8
9
10
11
12
13
14
15
16
17
18
19
20
21
22
23
24
25
26
27
28
29
30
31
32
33
34
35
36
37
38
39
40
41
42
43
44
45
46
47
48
49
50
51
52
53
54
55
56
57
58
59
60

1
2
3 resulted 98% conversion using just two mmol of the Et₃N base. Seeking similar results in this
4 current work, the hydrogenation reactions were performed with **4** at 0.1 mol% catalyst
5 loading for 2 h while varying the amount of Et₃N used. From **Figure 3**, it can be seen that as
6 the amount of base was decreased, the conversion also decreased slightly, with the highest
7 conversion being 99% for both 7.5 mmol and 5.0 mmol of base whereas 2.5 mmol of base
8 gave a conversion of 87%. All the reactions, however, gave 100% selectivities to FFA. When
9 the reaction was performed without base, no conversion was observed. Hence, 5.0 mmol of
10 base was selected as the optimum amount of base and was thus used for further reactions.
11
12
13
14
15
16
17
18
19
20
21
22
23
24
25
26
27
28
29
30
31
32
33
34
35
36
37
38
39
40
41
42
43
44
45
46
47
48
49
50
51
52
53
54
55
56
57
58
59
60

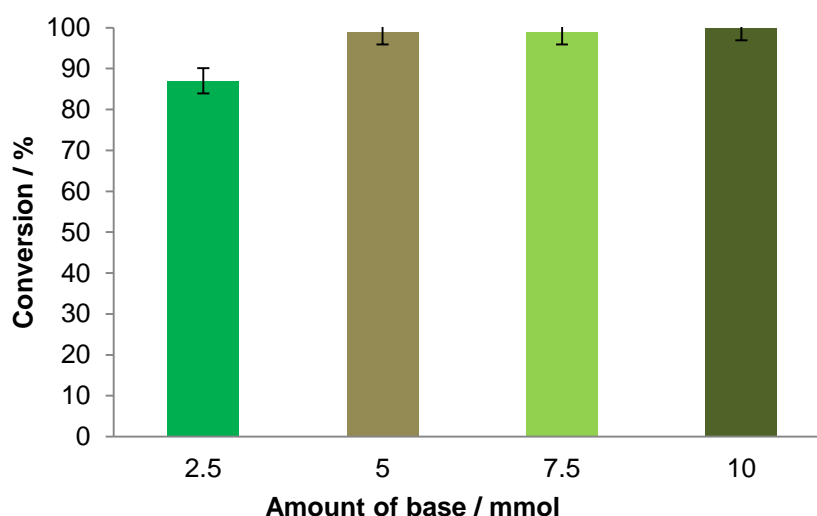


Figure 3: Conversion as a function of base

Conditions: FFR (20 mmol), formic acid (20 mmol), catalyst (0.02 mmol), 2 h, 140 °C. [a]

Conversion and Selectivity determined by NMR spectroscopy.

3.2.2 Catalyst loading

The catalyst loading was varied using 5.0 mmol of base (**Figure 4**). As the amount of catalyst was reduced, conversion of FFR also reduced. 0.075 mol% and 0.05 mol% of catalyst both gave conversions of 98 % whereas 0.025 mol% gave a conversion of 74 % with a TON and TOF of 2961 and 1481 h⁻¹ respectively. O'Connor and co-workers used 1 mol% of an iridium half-sandwich catalyst precursor to reduce FFR to FFA in 95 % yield within half an hour.³⁰ In this work, the amount of iridium half-sandwich catalyst precursor used was twenty times less (0.05 mol%) but still resulted in a relatively higher conversion of FFA, *albeit* in 2 hours. This

reduction in amount of catalyst is potentially a more economical way to offset the high cost of iridium metal. A catalyst loading of 0.05 mol% was hence selected as the optimum amount of catalyst for the reaction where a TON and TOF of 1964 and 982 h⁻¹ was recorded.

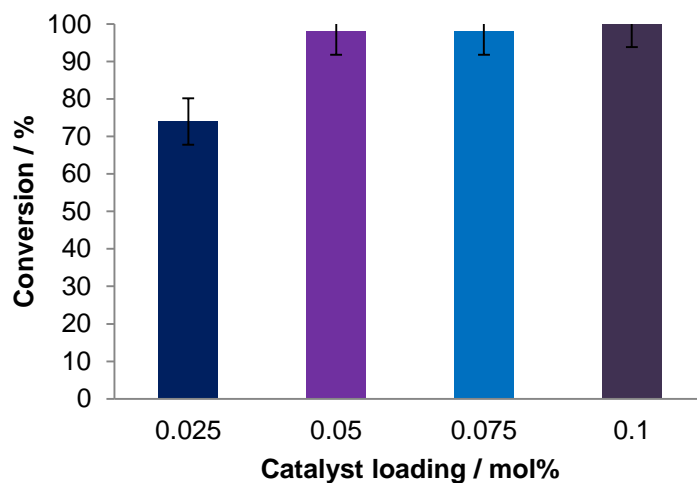


Figure 4: Catalyst loading

Conditions: FFR (20 mmol), formic acid (20 mmol), base (5 mmol), 2 h, 140 °C. [a] Conversion and Selectivity determined by NMR spectroscopy.

3.2.3 Homogeneity test

In order to test the homogeneity of the active catalyst in the hydrogenation of furfural to furfuryl alcohol, a mercury poisoning test was performed with catalyst **4**. The reaction was performed with 20 mmol of FFR, 20 mmol of formic acid and 5 mmol of Et₃N at a catalyst loading of 0.1 mol%. Then, 330 mg of metallic mercury was added into the reaction vessel and the reaction was carried out for 2 h at 140 °C. Nanoparticles, formed during the reaction, could be responsible for the high activities observed, rendering the catalytic transformation to be classified as heterogeneous or even a cocktail of both heterogeneous and homogeneous catalysts.³⁹ A fast way of testing the true nature of the catalysts involved in the transformation is by the mercury poisoning test which is based on the ability of mercury(0) to amalgamate zero-valent metals or to adsorb them onto the metal surface.^{40,41} As such, to test for the homogeneity of our reactions, metallic mercury was added in order to poison any nanoparticles which could be formed during the reaction. At the end of the reaction, the selectivity remained 100% while the conversion of furfural had only reduced from 93% to 92%. This showed that the active species driving the catalysis is of a homogeneous nature.

3.2.4 Recyclability studies

View Article Online
DOI: 10.1039/D0NJ01811B

The recyclability of complex **4** was studied at 140 °C using 0.1 mol% catalyst loading, 20 mmol FA and 10 mmol of Et₃N over 2 h. At the end of the reaction, ethanol was added to the crude mixture, in the autoclave reactor, to dissolve its contents. The liquids (including products and solvent) were removed under vacuum at 100 °C, leaving behind a solid residue, which was dried overnight in a vacuum oven, at 40 °C. The dried catalyst was transferred back into the reactor and recharged with FFR, FA and Et₃N before heating at 140 °C for 2 h. The procedure was repeated until the eighth run (**Figure 5**). The first run gave 100 % conversion of furfural and 100% furfuryl alcohol selectivity as expected, however, the furfural conversions of the subsequent runs reduced to greater than 90% (runs 2 and 3 recording 96%, 94% respectively). After the third run, the conversions further reduced to greater than 80% (runs 4, 5 and 6 recording 83%, 82% and 81% respectively). For the 7th run, the furfural conversion reduced to 75%. However, when the eighth run was attempted, the content of the reactor had dried up. The furfuryl alcohol selectivities recorded from run 2 through to run 7 were all greater than 95%.

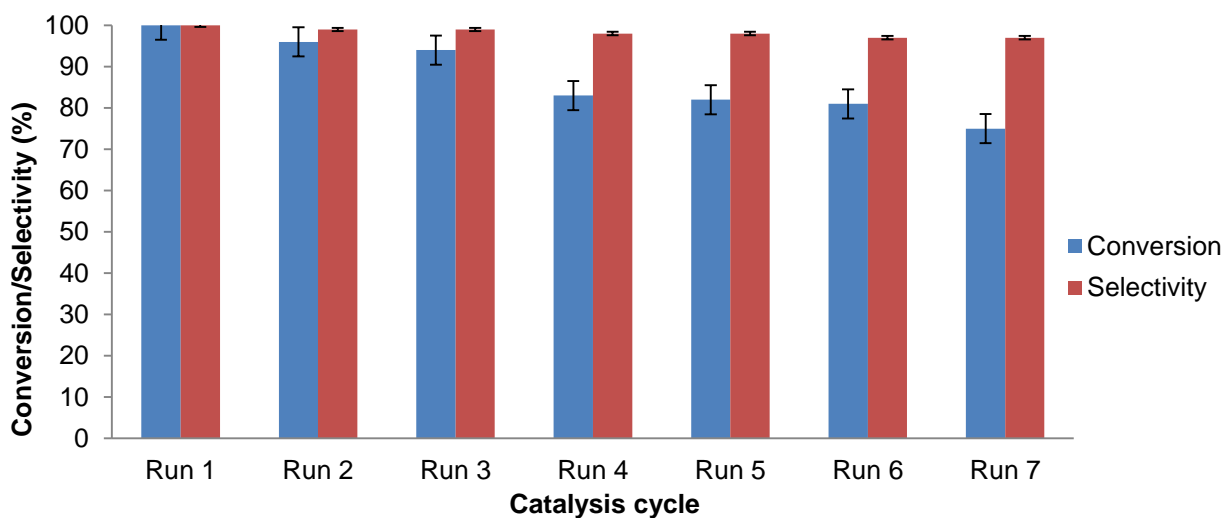


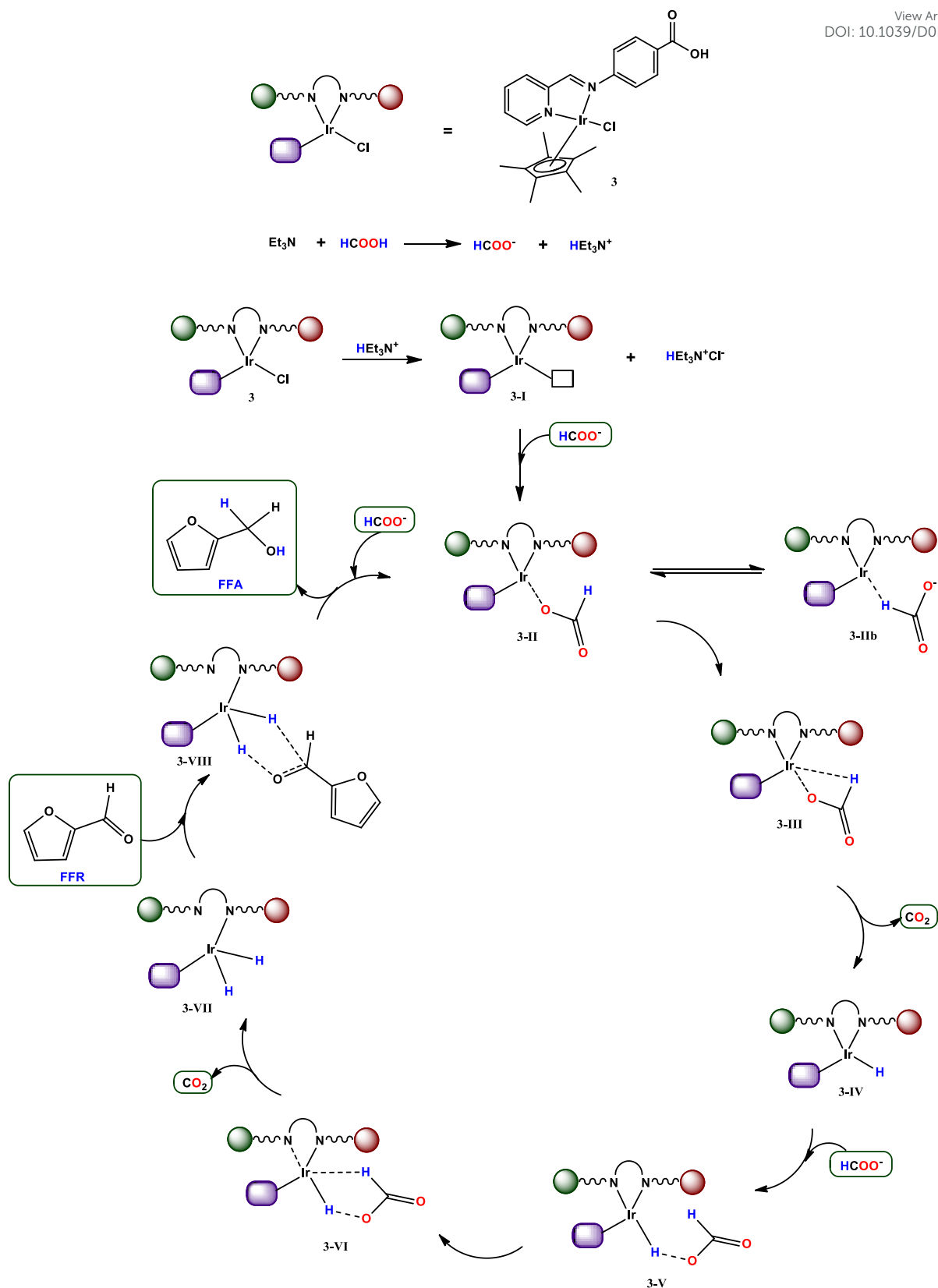
Figure 5: Recyclability of complex **4**

Conditions: FFR (20 mmol), formic acid (20 mmol), base (10 mmol), catalyst (0.02mmol), 2 h, 140 °C. [a] Conversion and Selectivity determined by NMR spectroscopy.

3.2.5 *In-situ* NMR spectroscopy studies

View Article Online
DOI: 10.1039/D0NJ01811B

A small scale reaction was performed in a J Young NMR tube by loading catalyst **3**, formic acid, Et₃N and MeOD₄ and monitoring the progression using NMR spectroscopy at 60 °C. After 30 mins, the ¹H NMR spectrum (**Figure S10**) showed the formation of iridium-hydride peaks. Chemical shifts appeared at -9.5 ppm and -10 ppm which correspond to a dihydride⁴² and a monohydride⁴³ species respectively. A dihydrogen species usually appears further downfield around -2 ppm as reported in literature,^{42,44} however this was not observed. In addition, there was no evidence of a hydrogen gas peak in the spectrum. Initially the two hydride species appear with the same intensity, however, as the reaction progresses, the monohydride (-10 ppm) reduces in intensity, while the dihydride (-9.5 ppm) increases in intensity. The dihydride however, appears as a sharp singlet instead of a doublet possibly due to the fact that the hydrides are in the same chemical environment. A similar observation was reported by Heinekey *et al.*, in their study of the structure of iridium Cp* complexes in which a single peak for their dihydride specie was seen.⁴⁵ In addition to these two hydride species, there is also a peak which appears at -9.6 ppm. Due to the low intensity of this peak, it is likely to be from a hydride with very little concentration in the system, possibly *via* a reversible pathway. There is also a new doublet peak at 8.8 ppm, which corresponds to the species in which the Ir-N_{pyridyl} bond has cleaved. The cleavage occurs at the pyridyl nitrogen and not the imine nitrogen bond because there was no new sharp singlet appearing between 8.5 ppm – 9 ppm (expected region of imine resonance of ligand **L1**) in the ¹H NMR spectrum. This is further supported by the molecular structure for **3**, where from its crystallographic, the Ir-N_{imine} bond (2.08 Å) is stronger than the Ir-N_{pyridyl} bond (2.12 Å).



Scheme 3: Proposed catalytic mechanism.

3.2.6 Proposed FFR hydrogenation mechanism

View Article Online
DOI: 10.1039/D0NJ01811B

The proposed reaction mechanism for the hydrogenation of (FFR to FFA with catalyst **3** is shown in **scheme 3**. The reaction begins with the deprotonation of formic acid by Et₃N to form a formate ion and a triethylammonium ion. A vacant coordination site is then created on the iridium metal (**3-I**) when the triethylammonium ion abstracts a chlorine atom to form a triethylammonium chloride salt. This allows coordination of the formate to the iridium metal to form species **3-II**. There is the likelihood of the formate ion coordinating to the iridium metal through the hydrogen atom to form a bridged Ir–hydride species as shown in **3-IIb**. This however, would be in minute concentrations if it were to occur since the negatively charged oxygen on the formate would form a better bond with the iridium metal. In lieu of this, **3-IIb** is likely to correspond to the hydride observed at -9.6 ppm. After expulsion of CO₂ from **3-II**, the iridium monohydride species **3-IV** is formed. A second coordination of a formate to **3-IV** and subsequent release of CO₂ leads to the formation of the iridium dihydride species **3-VII**, which is the active species. Iridium assisted transfer of the hydrogen atoms to **FFR** to form **3-VIII** is followed by the release of **FFA** and coordination of a formate to form intermediate **3-II**.

4. CONCLUSION

We have shown that iridium and ruthenium half sandwich complexes can be used successfully as catalyst precursors in homogeneous hydrogenation of furfural to chemoselectively produce furfuryl alcohol, in a short period of time. The iridium complexes performed better than their ruthenium analogues in terms of selectivity to furfuryl alcohol. The efficiency of these complexes can be seen in the results obtained, a turnover number of 2961 and turnover frequency of 1481 h⁻¹ as well as the maintenance of this high activity even after it was recycled seven times. The recyclability of the catalyst, the fact that the hydrogenation reaction was performed under solvent-free conditions and use of a safer alternative to molecular hydrogen makes the catalytic process presented herein a greener pathway of synthesizing furfuryl alcohol.

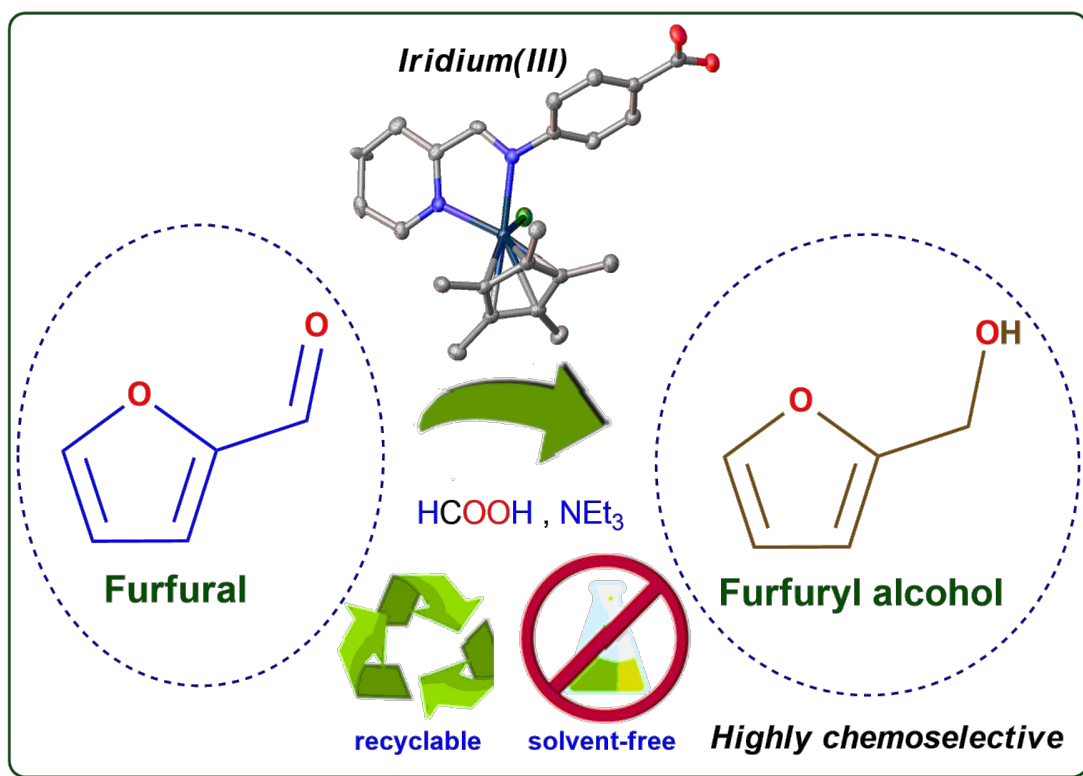
5. REFERENCES

View Article Online
DOI: 10.1039/D0NJ01811B

- 1 L. R. Lynd, C. E. Wyman and T. U. Gerngross, *Biotechnol. Prog.*, 1999, **15**, 777–793.
- 2 M. M. Ahmed, N. S. Nasri and D. U. Hamza, *Int. J. Eng. Sci. Technol.*, 2012, **4**, 721–730.
- 3 C. Briens, J. Piskorz and F. Berruti, *Int. J. Chem. React. Eng.*, 2008, **6**, 1–52.
- 4 M. J. Climent, A. Corma and S. Iborra, *Green Chem.*, 2014, **16**, 516–547.
- 5 T. Werpy and G. Petersen, *Top Value Added Chemicals from Biomass Volume I—Results of Screening for Potential Candidates from Sugars and Synthesis Gas*, Springfield, VA 22161, 2004.
- 6 J. J. Bozell and G. R. Petersen, *Green Chem.*, 2010, **12**, 539–554.
- 7 A. Fuente-Hernandez, R. Lee, B. Nicolas and I. Zamboni, *Energies*, 2017, **10**, 286–296.
- 8 A. Fuente-Hernández, P. Corcos, R. Beauchet and J. Lavoie, in *Liquid, Gaseous and Solid Biofuels - Conversion Techniques*, ed. Z. Fang, InTech Open, 2013, pp. 3–46.
- 9 R. Mariscal, M. Ojeda, P. Maireless-Torres, I. Sadaba and M. L. Granados, *Energy Environ. Sci.*, 2016, **9**, 1144–1189.
- 10 X. Chen, L. Zhang, B. Zhang, X. Guo and X. Mu, *Nat. Publ. Gr.*, 2016, 1–13.
- 11 R. Rao, A. Dandekar, R. T. K. Baker and M. A. Vannice, *J. Catal.*, 1997, **171**, 406–419.
- 12 Á. O’Driscoll, J. J. Leahy and T. Curtin, *Catal. Today*, 2017, **279**, 194–201.
- 13 S. Sitthisa, T. Pham, T. Prasomsri, T. Sooknoi, R. G. Mallinson and D. E. Resasco, *J. Catal.*, 2011, **280**, 17–27.
- 14 S. T. Thompson and H. H. Lamb, *ACS Catal.*, 2016, **6**, 7438–7447.
- 15 W.-P. Wu, Y.-J. Xu, S.-W. Chang, J. Deng and Y. Fu, *ChemCatChem*, 2016, **8**, 3375–3380.
- 16 B. M. Nagaraja, A. H. Padmasri, B. D. Raju and K. S. Rama Rao, *Int. J. Hydrogen*

- Energy*, 2011, **36**, 3417–3425.
- 17 Y. Wang, D. Zhao, D. Rodríguez-Padrón and C. Len, *Catalysts*, ,
DOI:10.3390/catal9100796.
- 18 R. van Putten, J. Benschop, V. J. de Munck, M. Weber, C. Müller, G. A. Filonenko
and E. A. Pidko, *ChemCatChem*, 2019, **11**, 5232–5235.
- 19 S. Gladioli and E. Alberico, *Chem. Soc. Rev.*, 2006, **35**, 226–236.
- 20 B. He, P. Phansavath and V. Ratovelomanana-Vidal, *Org. Chem. Front.*, ,
DOI:10.1039/c9qo01514k.
- 21 X. Wu, J. Liu, X. Li, A. Zanotti-Gerosa, F. Hancock, D. Vinci, J. Ruan and J. Xiao,
Angew. Chemie - Int. Ed., 2006, **45**, 6718–6722.
- 22 E. Fujita, J. T. Muckerman and Y. Himeda, *Biochim. Biophys. Acta - Bioenerg.*, 2013,
1827, 1031–1038.
- 23 W.-H. Wang, Y. Himeda, J. T. Muckerman, G. F. Manbeck and E. Fujita, *Chem. Rev.*,
2015, **115**, 12936–12973.
- 24 J. Deng, Y. Wang, T. Pan, Q. Xu, Q.-X. Guo and Y. Fu, *ChemSusChem*, 2013, **6**,
1163–1167.
- 25 W. Li, J.-H. Xie, H. Lin and Q.-L. Zhou, *Green Chem.*, 2012, **14**, 2388–2390.
- 26 N. K. Oklu and B. C. E. Makhubela, *Inorganica Chim. Acta*, 2018, **482**, 460–468.
- 27 G. Amenuvor, J. Darkwa and B. C. E. Makhubela, *Catal. Sci. Technol.*, 2018, **8**, 2370–
2380.
- 28 G. Amenuvor, B. C. E. Makhubela and J. Darkwa, *ACS Sustain. Chem. Eng.*, 2016, **4**,
6010–6018.
- 29 J. M. Tukacs, M. Bohus, G. Dibo and L. T. Mika, *RSC Adv.*, 2017, **7**, 3331–3335.
- 30 T. M. Townsend, C. Kirby, A. Ruff and A. R. O'Connor, *J. Organomet. Chem.*, 2017,
843, 7–13.
- 31 A. S. Gowda, S. Parkin and F. T. Ladipo, *Appl. Organomet. Chem.*, 2012, **26**, 86–93.

- 1
2
3
4
5
6
7
8
9
10
11
12
13
14
15
16
17
18
19
20
21
22
23
24
25
26
27
28
29
30
31
32 F. Huang, W. Li, Q. Lu and X. Zhu, *Chem. Eng. Technol.*, 2010, **33**, 2082–2088, View Article Online
DOI: 10.1039/D0NJ01811B
- 33 M. D. Bhor, A. G. Panda, N. S. Nandurkar and B. M. Bhanage, *Tetrahedron Lett.*,
2008, **49**, 6475–6479.
- 34 Bruker-AXS, *APEX3 Ver. 2016.5-0 (including SAINT and SADABS)*, Madison,
Wisconsin, USA, 2016.
- 35 O. V. Dolomanov, L. J. Bourhis, R. J. Gildea, J. A. K. Howard and H. Puschmann, *J.*
Appl. Crystallogr., 2009, **42**, 339–341.
- 36 G. M. Sheldrick, *Acta Crystallogr. Sect. A Found. Crystallogr.*, 2015, **71**, 3–8.
- 37 G. M. Sheldrick, *Acta Crystallogr. Sect. C Struct. Chem.*, 2015, **71**, 3–8.
- 38 J. Li, L. Guo, Z. Tian, M. Tian, S. Zhang, K. Xu, Y. Qian and Z. Liu, *Dalt. Trans.*,
2017, **46**, 15520–15534.
- 39 V. P. Ananikov and I. P. Beletskaya, *Organometallics*, 2012, **31**, 1595–1604.
- 40 K. C. Campbell and J. S. Hislop, *J. Catal.*, 1969, **19**, 12–19.
- 41 J. A. Steckel, *Phys. Rev. B*, 2008, **77**, 1–13.
- 42 M. Findlater, W. H. Bernskoetter and M. Brookhart, *J. Am. Chem. Soc.*, 2010, **132**,
4534–4535.
- 43 M. D. Millard, C. E. Moore, A. L. Rheingold and J. S. Figueroa, *J. Am. Chem. Soc.*,
2010, **132**, 8921–8923.
- 44 J. M. Goldberg, K. I. Goldberg, D. M. Heinekey, S. A. Burgess, D. B. Lao and J. C.
Linehan, *J. Am. Chem. Soc.*, 2017, **139**, 12638–12646.
- 45 D. M. Heinekey, D. A. Fine, T. G. P. Harper and S. T. Michel, *Can. J. Chem.*, 1995,
73, 1116–1125.
- 51
52
53
54
55
56
57
58
59
60



A recyclable homogeneous iridium complex for the selective synthesis of furfuryl alcohol from furfural without additional solvent and hydrogen gas.